Nonlinear absorption and ultrafast dynamics process of gold nanorods

SHUANG CHEN[a], SUYING YANG[b], WENZHI WU[a], YACHEN GAO[a,*]
[a]*Electronic Engineering College, Heilongjiang University, Harbin, 150080, China*
[b]*Physics Group, Chaoyang Medical School, Chaoyang, 122000, PR China*

The nonlinear absorption of gold nanorods (GNRs) was investigated by nanosecond Z-scan technique at 532nm. It was found that the GNRs exhibit saturable absorption (SA) characteristics. The SA was ascribed to the bleaching of ground state plasmon. Besides, the ultrafast dynamics process of the GNRs was investigated by femtosecond pump-probe technology. It was found that the dynamics process includes a fast decay and a slow decay with time constant of 3ps and 105ps, respectively. Theoretical results show that the fast decay process is due to the coupling of electron-phonon, and the slow decay process is due to the coupling of phonon-phonon.

(Received March 11, 2019; accepted October 9, 2019)

Keywords: Saturable absorption, Dynamics process, GNRs, Z-scan, Pump-probe

1. Introduction

As an important part of nanomaterials, metal nanoparticles (especially gold and silver) have attracted more and more attention in recent years [1, 2], and have been widely used in plasmon waveguide [3], cancer hyperthermia [4] and so on. The excellent optical properties of noble metal nanoparticles are due to their surface plasmon resonance (SPR). The collective oscillations of the free electrons in metal that interact with electromagnetic fields are called SPR [5]. The optical properties of nanoparticle change with the composition, shape, size, and properties of surroundings [6, 7]. Compared to nanospheres and nanoshells, nanorods have tunability of SPR band from the visible range to near-infrared-region (NIR) of optical frequencies meanwhile maintaining the small size of nanoparticles [8, 9]. Thus GNRs may be used in many applications such as biological imaging [10-13], drug carrier and cancer hyperthermia [14, 15]. GNRs exhibit anisotropic optical properties, that is, there are two resonance peaks, longitudinal surface plasmon resonance (LSPR) and transverse surface plasmon resonance (TSPR) [16, 17]. In addition, the TSPR peak of GNRs is at 520 nm, while the LSPR is highly adjustable. The LSPR peak of GNRs can be modulated in a wide range near the infrared region by changing the aspect ratio of rod to diameter [18]. As far as we know, third-order nonlinear optical absorption properties of GNRs have been rarely reported. Elim et al studied nonlinear absorption of GNRs with femtosecond z-scan experiments at wavelength of 800 nm [19]. They found that, under lower excitation irradiances, GNRs appear as saturable absorbers near the SPR longitudinal mode, while the energy increase, reverse saturation absorption (RSA) is dominant. The SA was attributed to the bleaching of ground state plasmon band and the RSA was attributed to excited state absorption of material. Tsutsui et al. investigated third-order nonlinear coefficient of spheres, nanorods and nanorods with femtosecond z-scan and I-scan experiments at wavelength of 800 nm [20]. The absorption peaks of the nanoparticles correspond to 530 nm, 800 nm, and 1000 nm, respectively. They found that, the third-order nonlinear coefficient of GNRs is 45 times that of spherical gold nanoparticles. This is mainly due to the fact that the LSPR of the GNR coincides with the position of the excitation wavelength, resulting in the effect of resonance enhancement. Joanna Olesiak-Banska et al. studied nonlinear absorption of GNRs with femtosecond z-scan techniques at wavelength of 550-1550 nm [21]. The results show that the main cause of nonlinear absorption in the range of LSPR is the single photon saturation absorption, otherwise the main cause of nonlinear absorption in the range of TSPR is the two-photon absorption. L. De Boni and coworkers investigated nonlinear absorption of GNRs with picosecond Z-scan technology [22]. They found that, GNRs exhibit SA characteristics at low energy. However, in the high energy zone, the RSA of GNRs is caused by photodegradation. E. V. García-Ramírez et al. investigated nonlinear absorption of colloidal GNRs systems with picosecond z-scan techniques at wavelength of 532 nm and 1064 nm [23]. They found that, at 532 nm all samples exhibited SA, when the GNRs have LSPR near 1064 nm, SA can only be observed under low energy pulse experiments. While the samples exhibited RSA for both wavelengths under high energy pulse experiments. J. Li

and coworkers investigated anisotropic and enhanced nonlinear absorption of aligned GNRs embedded in a poly film with nanosecond z-scan experiments at wavelength of 800 nm [24]. They found that, the stretch process increases the nonlinear absorption coefficient by about 9 times and the anisotropy factor to about 20 times. R. West et al. investigated nonlinear absorption of GNRs with nanosecond z-scan experiments at wavelength of 532 nm [25]. They found that, GNRs exhibited RSA (optical limiting effects).

Recently, we have also studied the nonlinear absorption of GNRs with nanosecond open aperture z-scan experiments at wavelength of 532 nm. In contrast to what R. West has found, GNRs in our experiment exhibit SA characteristics. In addition, we studied the ultrafast dynamics process of GNRs.

2. Samples and experiments

The GNRs investigated in our experiments was obtained from Nanjing XFNANO Materials Tech Co., Ltd. The GNRs particles were examined by transmission electron microscopy (TEM). Linear optical absorption measurements were obtained with an ultraviolet − visible−near-infrared (UV−vis−NIR) spectrophotometer.

In Z-scan, the laser pulses used is provided by a frequency-double, Q-switched, mode-locked Continuum ns/ps Nd:YAG laser system, operating at 6ns pulses with 10 Hz repetition rate at 532 nm wavelength. The spatial distribution of the pulse is nearly a Gaussian profile. The open aperture Z-scan experiments on sample were conducted using typical set up [26]. In the Z-scan experiments, the focal length of the lens focusing on the laser beam is 308 mm, and the focal spot size is about 110 um. The laser pulses were focused on a quartz cuvette with a thickness of 2 mm which contained the GNRs solution. The linear transmittance of the solution is about 80% at 532 nm. The sample was mounted on a translation stage so that it can move precisely as it passes through the focus area of the laser beam. The incident and transmitted laser pulses for each z point are recorded by a computer.

In the view of applications, both the magnitude and response time of nonlinearity are essential for materials. The ultrafast dynamics process of GNRs was measured by pump-probe method. An amplified Ti: sapphire laser system providing 130fs, 800 nm laser was used in pump-probe experiment. The repetition rate of the laser was 1 kHz. A small portion of the fundamental was used to generate a probe light, the remaining laser light was frequency-doubled to obtain 400 nm excitation light. We use a prism mounted to adjust the pump-probe delay. The probe signal was recorded by using a digital lock-in amplifier. The motion of the delay stage was controlled by using a computer. The transient differential transmission $\Delta T(t)/T$ was acquired as a function of the temporal delay t between the pump and the probe.

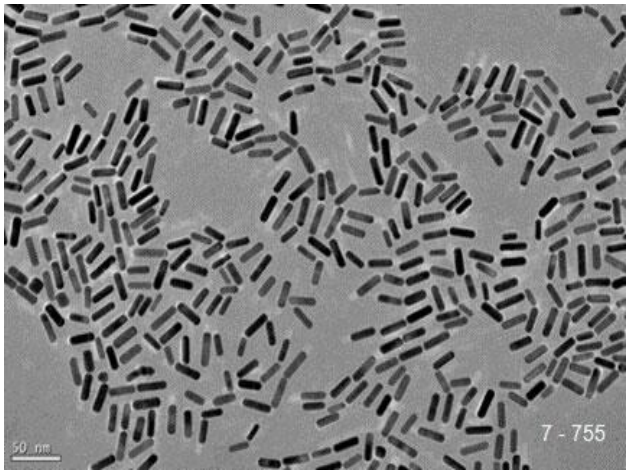

Fig. 1. TEM image of gold GNRs

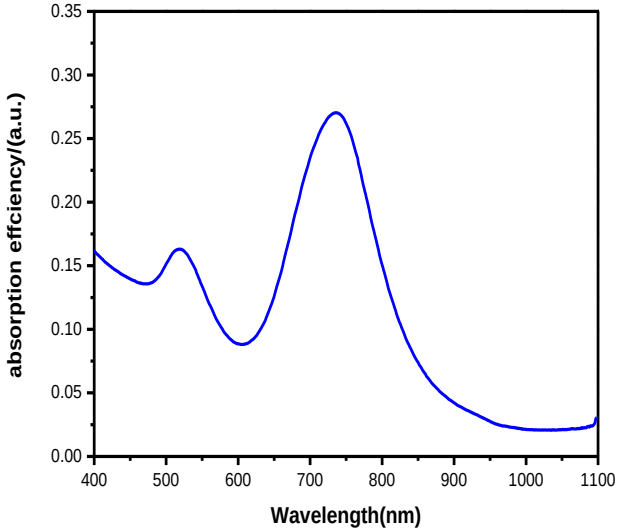

Fig. 2. Absorption spectrum of GNRs

3. Results and discussions

The TEM image of GNRs is shown in Fig. 1. It can be seen that the diameter of GNRs is about 5 nm and the length is about 30 nm. The absorption spectral of GNRs is shown in Fig. 2. It can be found that the GNRs have two absorption peaks at 520 nm and 755 nm respectively. The former is caused by a transverse mode perpendicular to the GNRs; the latter is caused by longitudinal mode perpendicular to the GNRs.

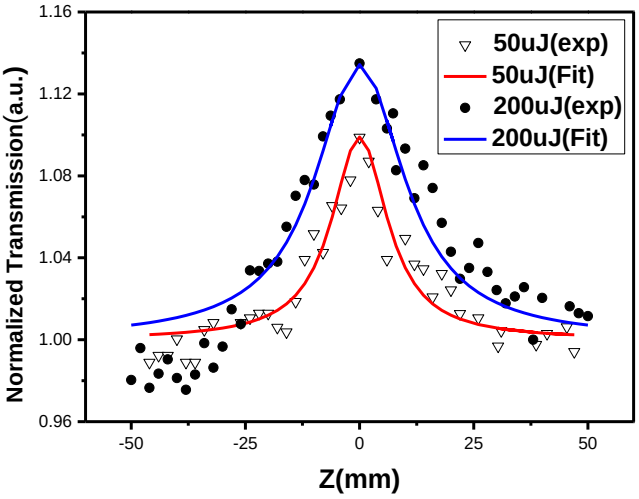

Fig. 3. Normalized transmission as a function of sample (GNRs) position for open aperture Z-scan at different intensities. The dots are experimental date while the solid lines are theoretical fit generated

Table 1. The saturation strength I_S obtained by calculated for the sample at different laser intensities

N_O	E （μJ）	I_0 （W/m^2）	I_s (W/m^2)
a	50	5.25×10^{12}	9×10^{11}
b	200	2.10×10^{13}	1.1×10^{12}

The open aperture Z-scan results of GNRs under different energies of 50 μJ, 200 μJ are shown in Fig. 3, a low repetition rate of 10Hz is chosen, thus the thermal effect can be ignored [24]. It can be found that the GNRs have the SA characteristics when the excitation intensities are different. Moreover, as the incident light energy increases from 50 μJ to 200 μJ, the transmittance of sample at focal point increases. When sample is far away from focal plane, the incident laser has a low irradiance and a constant transmittance. While sample is close to focal plane, the incident laser irradiance becomes larger, the transmittance increases, indicating an optically induced transparency in GNRs. The mechanism can be visualized as follows. As the absorption spectrum of GNRs shows a TSPR absorption band of 500-600 nm, excitation at 532 nm will prepare the system in the excited state. When irradiance is moderate, most of the GNRs are pumped to the excited state, resulting in a smaller number of the ground state which is called bleaching of ground state plasmon, which make the ground state absorption of the sample decrease.

Theoretically, when there is only two-photon absorption, the open aperture experimental curves were fitted by using the equation [26]:

$$T(z)=\sum_{m=0}^{\infty}\frac{[\frac{-\beta I_0 L_{eff}}{1+z^2/z_0^2}]^m}{(m+1)^{3/2}} \tag{1}$$

where $L_{eff}=(1-e^{-\alpha_0})/\alpha_0$, L_{eff} is the effective interaction length, β the nonlinear absorption coefficient, I_0 the peak intensity at the focus, z the displacement of the sample from the focus ($z=0$). L is the sample length, z_0 is the Rayleigh rang. But, when sample shows saturable absorption, in order to analyze the open-aperture Z-scan experimental data, Eq. (1) must be modified by replacing $\beta I_0/(1+z_2/z_0^2)$ in Eq. (1) by Eq. (2) as follows.

$$\alpha_0/\left[1+I_0/(1+z^2/z_0^2)I_s\right] \tag{2}$$

where α_0 is linear absorption coefficient, I_0 is laser intensity, I_S is saturable intensity. As shown in Fig. 3 using solid line, theoretical fit was made according to Eq. (1) and Eq. (2). The estimated values of saturation strength I_S are shown in Table 1. It can be seen from Table 1 that I_S increases with the increase of incident energy.

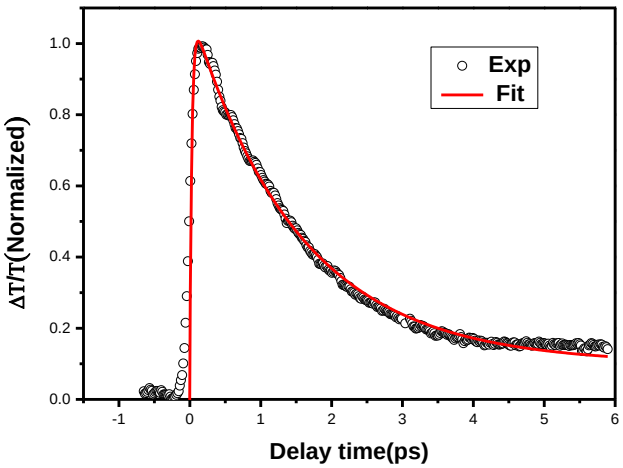

Fig. 4. Normalized transient differential transmission of pumping detection of GNRs. The open dots are experimental date while the solid lines are theoretical fit generated

Fig. 4 shows the normalized transient differential transmission $\Delta T(t)/T$ measured at pump power of 20 mw. It can also be found that, after intense laser excitation, a rapid rise process and two independent decay processes occurred. The rapid rise process is commonly referred to as plasma bleaching of the ground state of the system [27]. The large amount of the GNRs were pumped to the excited state, resulting in a small number of populations at the

ground state, this brought out the bleaching in the ground-state absorption band. Gold nanoparticles have inter-band transitions at 400 nm, so d-band electrons affect the results. Initially, optical pulse created electron-hole pairs at the excitation photon energy [28]. Because of the limited time resolution of our laser system we cannot accurately determine the processes. After the rapid rise process, $\Delta T(t)/T$ recovers on two different time scales and can be considered as two-exponential decay. The initial rapid decay is the excited electrons thermally balance with the nanoparticle lattice through electron–phonon interactions. The subsequent slow decay occurs when the phonon–phonon interactions with the surrounding medium.

In general, if only one decay occurs, the two-temperature model (TTM) can be used to interpret the process. Because there are two decay components in the current experiment. We used two e-exponential functions to fit the normalized transmittivity change:

$$\frac{\Delta T}{T} = A_1 \exp(-\frac{t}{\tau_1}) + A_2 \exp(-\frac{t}{\tau_2}) \quad (3)$$

where A_1, A_2 are the amplitudes of two decay components, τ_1 and τ_2 represents time constants of two decay components, repectively. The solid lines in Fig. 4 are theoretical fit generated. In this condition, the decay process are well fitted by the values of an initial rapid relaxation time and a slow relaxation time (τ_1 = 3ps, τ_2 = 105ps) [29]. In fact, the relaxation times (e-ph coupling time) in gold nanorods is longer than that reported in Au spheres (1ps) because gold nanorods have higher initial temperatures of hot electrons.

4. Conclusion

In summary, we have investigated the nonlinear absorption characteristics of GNRs at 532 nm. The results show that GNRs exhibit SA characteristics and the SA interpreted in the terms of ground state plasma bleach. Moreover, we have investigated ultrafast energy relaxation process of GNRs using 130fs laser pulses at 400 nm. We found that the relaxation processes contain two different time scales. The rapid one has the time constant is about 3ps corresponding to electron-phonon coupling, while the slower one is about 105ps corresponding to phonon-phonon coupling.

Acknowledgement

This work was supported by the Heilongjiang Province Natural Science Fund (F2018027). Science and Technology Project of Heilongjiang Education Department (11531283, 12511424). Heilongjiang University Graduate Innovation Fund (YJSCX2019-164HLJU).

References

[1] C. X. Kan, J. J. Zhu, X. G. Zhu, J. Phys. Chem. D **41**(15), 155304 (2008).
[2] J. A. Reyes-Esqueda, V. Rodríguez-Iglesias, H. G. Silva-Pereyra, C. Torres-Torres, A. L. Santiago-Ramírez, J. C. Cheang-Wong, A. Crespo-Sosa, L. Rodríguez-Fernández, A. López-Suárez, A. Oliver, Opt. Express **17**(15), 12849 (2009).
[3] S. A. Maier, P. G. Kik, H. A. Atwater, S. Meltzer, E. Harel, B. E. Koel, A. A. G. Requicha, Nat. Mater. **2**(4), 229 (2003).
[4] A. S. Thakor, J. Jokerst, C. Zavaleta, T. F. Massoud, S. S. Gambhir, Nano Lett. **11**(10), 4029 (2011).
[5] S. L. Qu, Y. L. Song, C. M. Du, Y. X. Wang, Y. C. Gao, S. T. Liu, Y. L. Li, D. B. Zhu, Opt. Commun. **196**, 317 (2001).
[6] Zheng, X. Huang, M. A. El-Sayed, J. Adv. Res. **1**, 13 (2010).
[7] V. Myroshnychenko, J. Rodríguez-Fernández, I. Pastoriza-Santos, A. M. Funston, C. Novo, L. M. Liz-Marzán, F. J. G. Abajo, Chemical Society Reviews **37**(9), 1792 (2008).
[8] K. S. Lee, M. A. El-Sayed, J. Phys. Chem. B **109**, 20331 (2005).
[9] W. Ni, X. Kou, Z. Yang, J. F. Wang, ACS Nano **2**, 677 (2008).
[10] J. Qian, L. Jiang, F. Cai, D. Wang, S. He, Biomaterials **32**, 1601 (2011).
[11] J. L. Li, M. Gu, Biomaterials **31**, 9492 (2010).
[12] X. Huang, I. H. El-Sayed, W. Qian, M. A. El-Sayed, J. Am. Chem. Soc. **128**(6), 2115 (2006).
[13] N. J. Durr, T. Larson, D. K. Smith, B. A. Korgel, K. Sokolov, A. Ben-Yakar, Nano Lett. **7**, 941 (2007).
[14] X. Huang, S. Neretina, M. A. El-Sayed. Adv. Mater. **21**, 4880 (2009).
[15] Z. Zhang, J. Wang, C. Chen, Theranostics **3**, 223 (2013).
[16] H. Baida, D. Mongin, D. Christofilos, G. Bachelier, A. Crut, P. Maioli, N. Del-Fatti, F. Vallée, Phys. Rev. Lett. **107**(5), 057402 (2011).
[17] E. V. García-Ramírez, S. Almaguer-Valenzuela, O. Sanchez-Dena, O. Baldovino-Pantaleon, J. A. Reyes-Esqueda, Opt. Express **24**(2), A154 (2016).
[18] C. J. Murphy, L. B. Thompson, A. M. Alkilany, P. N. Sisco, S. P. Boulos, S. T. Sivapalan, J. Huang, J. Phys. Chem. B **1**(19), 2867 (2010).
[19] H. I. Elim, J. Yang, J. Y. Lee, J. Mi, W. Ji, Appl. Phys. Lett. **88**, 083107 (2006).
[20] Y. Tsutsui, T. Hayakawa, G. Kawamura, M. Nogami, Nanotechnology **22**(27), 275203 (2011).
[21] J. Olesiak-Banska, M. Gordel, R. Kolkowski, K.

Matczyszyn, M. Samoc, J. Phys. Chem. C **116**(25), 13731 (2012).
[22] L. De Boni, E. L. Wood, C. Toro, F. E. Hernandez, Plasmonics **3**(4), 171 (2008).
[23] E. V. García-Ramírez, S. Almaguer-Valenzuela, O. Sánchez-Dena, O. Baldovino-Pantaleón, J. A. Reyes-Esqueda, Opt. Express **24**(2), A154 (2016).
[24] J. Li, S. Liu, Y. Liu, F. Zhou, Z.-Y. Li, Appl. Phys. Lett. **96**(26), 263103 (2010).
[25] R. West, Y. Wang, T. Goodson III, J. Phys. Chem. B **107**(15), 3419 (2003).
[26] M. Sheik-Bahae, A. A. Said, Van Stryland, E. W. IEEE J. Quantum Electron. **26**, 760 (1990).
[27] N. D. Fatti, F. Vallee, C. Flytzanis, Y. Hamanaka, A. Nakamura, Chem. Phys. **251**(1), 215 (2000).
[28] K. J. Prashan, W. Qian, M. A. El-Sayed, J. Phys. Chem. B **110**(1), 136 (2006).
[29] C. Y. Chen, J. Wang, S. Y. Yang, W. W. Wu, D. G. Kong, Y. C. Gao, Journal of Nanoparticle Research **20**(9), 242 (2018).

*Corresponding author: gaoyachen@hlju.edu.cn